










3D Modeling for Multimodal Visualization of Medical Data

Hayssam A. A. Obeid^{1,3,4} , Rita Zrou^{1,3} , Bruno Mercier^{1,3} , Sebastien Horna^{1,3} , Carole Guillevin^{2,3} , Mathieu Naudin^{2,3} , Mohamad Khalil⁴ 

¹XLIM laboratory, UMR CNRS 7252, University of Poitiers, France, author@univ-poitiers.fr

²LMA laboratory, UMR CNRS 7348, University of Poitiers, France, author2@chu-poitiers.fr

³I3M, Commun Laboratory CNRS-Siemens, University and Hospital of Poitiers, France,

⁴AZM center for research in biotechnology and its applications, Lebanese University, Lebanon,

Corresponding author: Hayssam A. A. Obeid, hayssam.abd.alaziz.obeid@univ-poitiers.fr

Abstract. Magnetic resonance imaging (MRI) is a medical imaging technique used in radiology to produce anatomical images and physiological information of the brain. Based on the principle of magnetic resonance, this non-invasive tool provides numerous types of advanced acquisitions. Some of these acquisitions can provide information on the concentrations of molecules within a well-localized volume in the cortex. Several studies have shown the important role of modeling and visualizing these concentrations according to brain anatomy and in high resolution to improve the diagnosis and treatment of tumor areas.

To visualize this data, physicians use the concentrations estimated after an acquisition in a grid composed of large voxels. In this acquisition grid, each voxel has a concentration value distributed evenly over its entire 3D space. Interpolation algorithms are usually applied on this grid in order to improve the spatial resolution. However, none of them takes into account the anatomical composition of the acquisition volume, which is a mixture of three substances that constitute a brain for a healthy subject, while in the case of a tumor subject, it also includes the presence of a tumor. These partial volumes, which make up the acquisition volume, admit very different molecular concentrations.

In this work, we present a multimodal process that allows us to model molecular concentrations, taking into account the heterogeneity of the tissues making up the acquisition volume. This process also makes it possible to visualize it in a higher resolution and in 3D. This new method ensures a better distribution of molecular concentrations by considering the real nature of the underlying tissues. It is based on distribution rates evaluated in clinical studies and corrects the effect of partial volumes of brain substances in the entire acquisition volume.

Keywords: 3D Modeling of Medical Data, Multimodal Visualization, Multiresolution, Magnetic Resonance Imaging

DOI: <https://doi.org/10.14733/cadaps.2024.778-790>

1 INTRODUCTION

Conventional magnetic resonance imaging (cMRI) is a medical imaging technique that provides non-invasive views of the interior of the brain with relatively high contrast resolution. It has become the most important diagnostic tool for brain tumor detection, planning and evaluation of treatment response [3, 10]. However, its ability to differentiate tumor types is limited and may lead to ambiguous results in some cases [7]. Therefore, advanced magnetic resonance imaging techniques have been integrated into clinical routine. These techniques provide important structural, functional, and metabolic information at the cellular level, highlighting aspects of brain pathophysiology [1, 11]. One of these techniques allows non-invasive exploration of the molecular composition of tissues and allows the identification of multiple molecular constituents in a well-localized volume of the cortex [4, 14].

The additional information provided by this advanced magnetic resonance imaging technique, which is represented by molecular concentration values, allows to characterize the metabolic profiles (concentration value of a set of molecules) in the brain, and to answer a number of important research questions [9]. These concentration values are particularly helpful for identifying different types of brain tumors, assessing their extent and invasion into neighboring tissues, and determining the best treatment for each patient. By comparing pre- and post-treatment concentrations, physicians can also monitor the effectiveness of treatment. Therefore, visualizing molecular concentration values obtained after acquisition within a higher resolution is essential for an accurate diagnosis, an effective treatment, and an understanding of brain functions and diseases [20].

To visualize molecular concentrations, physicians use the values estimated after acquisition in a regular grid composed of large subdivision volumes, which are referred to as macrovoxels in this article, each with a single value over its entire 3D space for each recorded molecule. Molecular concentrations are usually acquired with a large voxel size, which limits their spatial resolution. Regrettably, the acquisition grid's spatial resolution is determined by several factors, including imaging duration and the desired signal-to-noise ratio. Thus, to achieve an acquisition time acceptable to the patient and a satisfactory signal-to-noise ratio, physicians need to expand the volume of acquisition voxels. The low resolution of such acquisition can be increased by using post-processing techniques called super-resolution (SR) algorithms [12]. These methods are based on resampling the concentrations of molecules in another finer grid by interpolation. Classical interpolation algorithms can be applied to this acquisition grid to improve the spatial resolution and refine the details.

However, none of the existing algorithms account for the complex composition of the acquisition volume, which encompasses a blend of three distinct substances forming the brain in a healthy individual and incorporates a tumor area in patients with tumors [15]. Combining this advanced MRI technique with anatomical data, represented by the three brain substances: white matter (WM), gray matter (GM) and cerebrospinal fluid (CSF), as well as the tumor area in patients, can help solve difficult cases and increase diagnostic confidence [16]. Therefore multimodal visualization of the anatomical data with the concentrations of the molecules in a single rendering remains a challenge compared to the usual use of several processing softwares. It is necessary to propose a system for visualizing all this complex information resulting from different types of acquisition by combining and by synthesizing them in a single rendering which represents several modalities at the same time. This system allows doctors to visualize this information, to facilitate cross-checking between the different data and thus to make more reliable diagnoses when predicting the onset of certain diseases, in particular tumors with a classification of its grade.

In this paper, we present a multimodal method of molecular concentration modeling that takes into account the heterogeneity of tissues in an acquisition volume. This method presents an automatic process to integrate the concentrations of molecules into high-resolution anatomical images by quantifying its values in the partial volumes of the tissues in each macrovoxel of interest. This allows better modeling and distribution of the molecular concentration, giving weight to the real nature of the underlying tissues according to the distribution rates evaluated in clinical studies (Fig. 1). We present their results, advantages, and limitations. All our developments, tests and comparisons are carried out in the open-source software 3D Slicer [5].

This paper is organized as follows. In section 2 we present the existing method to visualize the concentration of a molecule. In section 3, we present a new method for modeling and visualizing in 3D concentrations, combined with the anatomical data, then the results after the application of our method on a healthy subject. In section 4 we present the extension and the results of our algorithm to treat a tumor subject. In section 5 we interpret the results obtained, and we evaluate the effectiveness of the process compared to the existing method. Finally, section 6 states the conclusion and some perspectives.

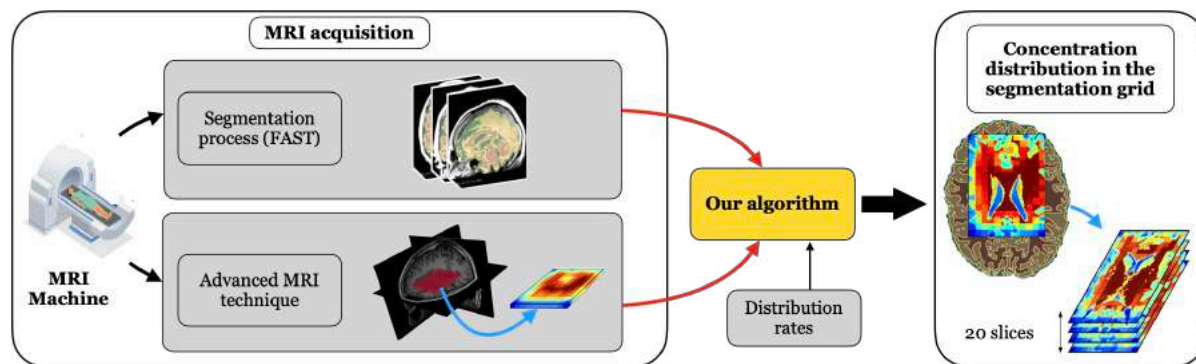


Figure 1: The processing flow: Our algorithm uses the data provided by the MRI acquisition system (the anatomical structures and the concentrations of the molecules) to calculate, according to the distribution rates, the new distribution of the concentrations in the resolution of the segmentation grid.

2 STANDARD MODELING METHOD

In this section, we present the existing method to visualize the concentration of a molecule in a regular grid well localized in the healthy brain, representing the region where the acquisition was made (Fig. 2-(b)). In order to visualize the data, two grids are considered. The first is the acquisition grid formed of the large macro voxels where the molecular concentration was estimated after the acquisition (Fig. 2-(a)). This lower spatial resolution grid is obtained with a large volume of macrovoxels, typically $7*7*20 \text{ mm}^3$, each of them contains a concentration value (for each molecule) uniformly distributed over its entire 3D space. Practical limitations of available scan time place major constraints on this type of data in terms of image resolution. In order to reduce the acquisition time and to limit the increase of artifacts in the estimated data, the volume of the macrovoxels is increased. An acquisition of molecular concentrations with a large macro voxel size allows a reasonable acquisition time for the patient but degrades the analysis of tissue microstructural features [2].

The second grid considered is the segmentation grid obtained by a specific acquisition and segmentation process, which aims to initialize the nature of its voxels (called microvoxels). In this study, we initialized the nature of each micro voxel in the segmentation grid using the FAST software, which is a commonly used tool for segmenting T1-weighted brain MRI images into several tissue types: white matter, gray matter, cerebrospinal fluid, and tumor area (for patients with tumors) [17]. The segmentation process using this software involves running the segmentation algorithm to generate tissue probability maps for the brain substances. Subsequently, a threshold is applied to each tissue probability map, resulting in the generation of binary masks for each tissue type (Fig. 2-(c)). This higher spatial resolution grid is obtained with a much smaller volume of microvoxels, typically $1*1*1 \text{ mm}^3$, each of them belonging to one of the substances that make up the brain [6].

A super-resolution (SR) approach is a technique used to improve the resolution and detail of the originally acquired data. The primary concept behind SR is to initialize the concentration value of each microvoxel in the segmentation grid based on its corresponding macrovoxel, where it belongs, and its neighboring macrovoxels.

This is achieved through the application of a standard bilinear interpolation operation. These interpolation algorithms cannot fix the effect of partial volumes of brain substances in the acquisition volume, which has the potential to introduce error when quantifying molecular concentration [12]. Moreover, the thickness of the acquisition grid being a single macrovoxel, the interpolation is finally performed only in 2D (Fig. 2-(b)). Conventional interpolation methods available in most processing tools are based on basic mathematical operations that are applied directly to images, regardless of brain composition. These algorithms fail to consider the variability within a macrovoxel volume that is composed of multiple tissue compartments.

For this type of quantitative data, that are stored in a matrix (in the acquisition grid) and represented as an image (like a heat map), it cannot be assumed that they are like simple images containing simple values to which we can apply image processing operations. These values are concentrations of molecules in an acquisition volume, and one must interact with them as quantitative parameters. Therefore, the use of visualization and interpolation algorithms that do not account for this specific data leads to inaccurate concentration quantification that is difficult for physicians to interpret.

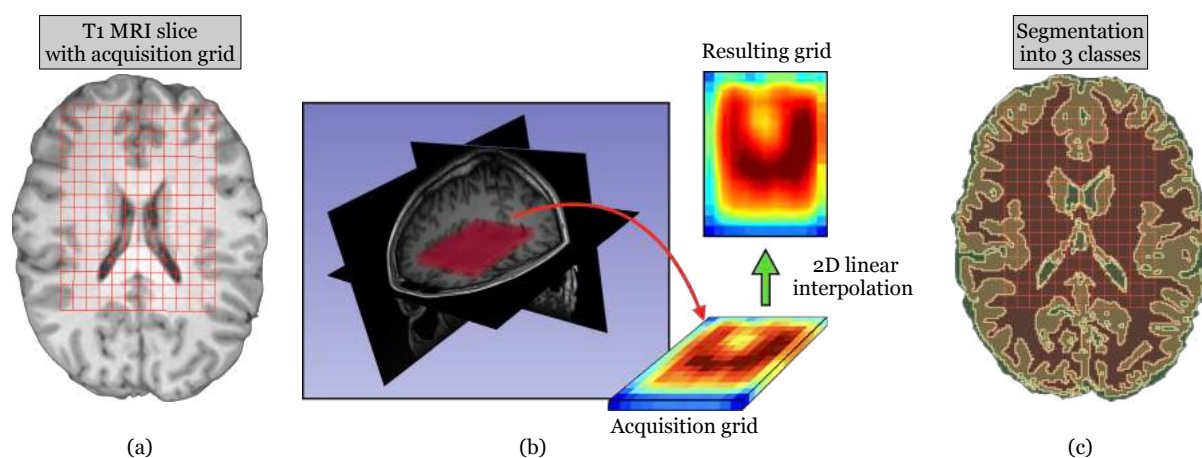


Figure 2: Standard Modeling Method: (a) acquisition grid [red colored] localized on a T1 MRI slice; (b) 3D view of the acquisition grid into the brain [red colored] and the concentration distribution for only one molecule inside it, the concentration distribution in the segmentation grid after applying the linear interpolation on the estimated concentration values: from the higher concentration [dark red colored] to the lower concentration [dark blue colored]; (c) acquisition grid [red colored] localized on a MRI slice segmented into three brain substances: cerebrospinal fluid mask [green colored], white matter mask [brown colored] and gray matter mask [yellow colored].

3 NEW PROPOSED MODELING METHOD

Studies based on the adjustment of acquisition parameters in the clinical setting show that the molecules are not uniformly distributed among the three brain substances. In general, white matter, which is primarily composed of axons, has lower levels of these molecules compared to gray matter, which is rich in cell bodies and dendrites. The cerebrospinal fluid, which surrounds the brain and spinal cord, also contains these molecules, but at much lower levels than in white or gray matter. The doctors succeeded in determining the distribution rates of the molecules in each brain substance. These values determine how each molecule is distributed among substances in the brain: these distribution rates are constant despite variations in molecular concentrations from one patient to another [21]. Our modeling algorithm aims to estimate the concentration of a molecule in

the microvoxel resolution according to their tissue nature, the overall concentration of the macrovoxel where they are included, and the distribution rates assessed in the clinical setting. This is achieved by computing, for each macro voxel, the concentration in each of the volumes of the substances that form it. In the following, we explain how the algorithm is applied to a healthy macro voxel. The same steps are applied for each macro voxel not affected by a disease of the acquisition grid.

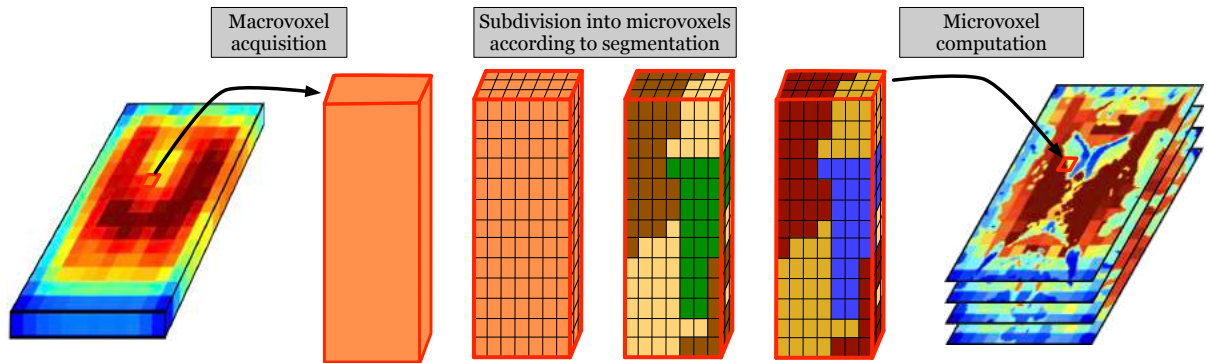


Figure 3: Our new Modeling Method: macrovoxel acquisition estimates concentration values of a molecule in a very thick 12x16 resolution grid; Subdivision into microvoxels cuts each macrovoxel in order to obtain a grid as refined as the acquired MRI T1 slices. The segmentation method is used to classify each microvoxel according to its substance (white matter, gray matter or cerebrospinal fluid); The new concentration, according to anatomy is evaluated during the microvoxel computation by using the distribution rates of the literature.

For each macro voxel, the process gives: its volume V (unit of volume) typically $7*7*20 \text{ mm}^3$ and the concentration C of a molecule X (unit of quantity/volume) inside, obtained after the acquisition. These macro voxels were divided into small voxels having the same dimensions as the micro voxels of the segmentation grid. Based on the anatomical data already stored in the segmentation grid after the application of the segmentation tool and the position of the macro voxels in the cortex, the nature of these voxels can be initialized: each is marked by gray matter, white matter or cerebrospinal fluid (see Fig. 3 for an overview of the process). Obviously, we cannot make the assumption that the concentration C is uniform across all the voxels that compose a macro voxel, especially since these individual voxels may be associated with different types of tissue, each with its own concentration level. The purpose is to evaluate the concentration of X in these three substances that we note respectively C_1 , C_2 and C_3 . The concentration of X in each partial volume of brain substances in a macrovoxel depends on its concentration C , the volumes of each substance in this macrovoxel, and the rates of tissue distribution. The computation of the volumes of these substances in a macrovoxel is done by counting the number of voxels for each substance and then multiplying by the volume of a microvoxel, typically $1*1*1 \text{ mm}^3$. The volumes of three substances in the macrovoxel are respectively denoted V_1 , V_2 , and V_3 for the substances 1, 2 and 3. The distribution rates of X in the three cerebral substances are noted respectively a_1 , a_2 and a_3 (constant values).

The mass of the molecule X in each macrovoxel is equal to $C * V$. This mass is well distributed between the three substances in a non-uniform way but it is always conserved (Eq. 1).

$$C * V = C_1 * V_1 + C_2 * V_2 + C_3 * V_3 \quad (1)$$

The concentrations of the molecule X in each substance are related to the distribution rates by the following equations:

$$a_2 * C_1 = a_1 * C_2 \quad (2)$$

$$a_3 * C_2 = a_2 * C_3 \quad (3)$$

$$a_1 * C_3 = a_3 * C_1 \quad (4)$$

By replacing the concentration C_2 and C_3 by their value as a function of C_1 in Eq. 1, we obtain the concentration C_1 in a volume V_1 as follows:

$$C_1 = \frac{C * V}{V_1 + \frac{a_2}{a_1} * V_2 + \frac{a_3}{a_1} * V_3} \Rightarrow C_1 = \frac{a_1 * C * V}{a_1 * V_1 + a_2 * V_2 + a_3 * V_3} \quad (5)$$

C_2 and C_3 are deduced from C_1 using equations (2), (3) and (4). After estimating the concentration of a molecule X in each volume V_i , it is assumed that X is uniformly distributed in each volume V_i and the concentration of X in each voxel is initialized by the concentration values C_i estimated according to the nature of the tissue that composes it. Then the concentration in each voxel of volume V_i is initialized by C_i . Fig. 4 and Fig. 5 show the results of applying our modeling method to a healthy subject.

A Gaussian filter in 3D and by substance was applied to the concentration values in the segmentation grid after applying our method [13, 19]. This can be useful in situations where the image contains noise or other artifacts from the segmentation process. By applying the filter to each substance separately, the calculated concentration values can be smoothed without affecting those of other substances, resulting in more accurate and reliable estimated concentrations (Fig. 5).

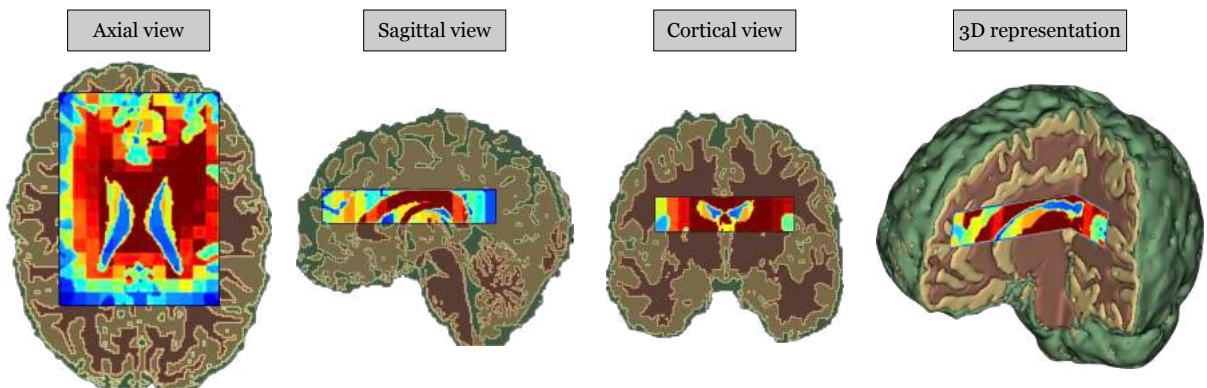


Figure 4: Three views of the molecular concentration slices in the segmentation grid with the corresponding brain substance masks after applying our method. A multimodal 3D visualization is obtained (on right): concentration values merged with brain substances.

Clinical research has been conducted to investigate how the concentration of a specific molecule varies across different brain substances for healthy subjects. The objective of this research is to gain a better understanding of the molecule's normal distribution in the brain. The results suggest that the molecule is distributed within a specific range in each type of brain substance. This variation within the same substance can be attributed to the location of the acquisition volume in the brain. Therefore, the concentration value of the molecule depends not only on the type of tissue but also on its specific location within the brain [18]. To further validate our algorithm, we examined the concentration variation of each recorded molecule within each cerebral substance after applying our algorithm. To achieve this, we initially selected microvoxels with white matter characteristics in the acquisition volume. Subsequently, we analyzed the estimated concentration variation using our algorithm of each molecule in these microvoxels. This same process was performed on microvoxels with gray matter features. The information presented in Tab. 1 displays the fluctuations in concentration for three different molecules (Choline (CHO), Creatine (Cr), and N-acetyl aspartate (NAA))

as measured by both our method and the methods described in [21], in both the white matter and the gray matter (the two substances for which the concentrations are the most significant). We can remark that the estimated concentration variations are quite similar to those reported in clinical studies [15, 21], and that the differences between the different tissues are consistent (same difference between gray matter and white matter, same standard deviation in the substances for each molecule). This suggests that the results obtained from the study data are reliable and representative of reality. In other words, the precision of the concentration estimates and the consistency between the tissues reinforce the validity of the results of clinical studies.

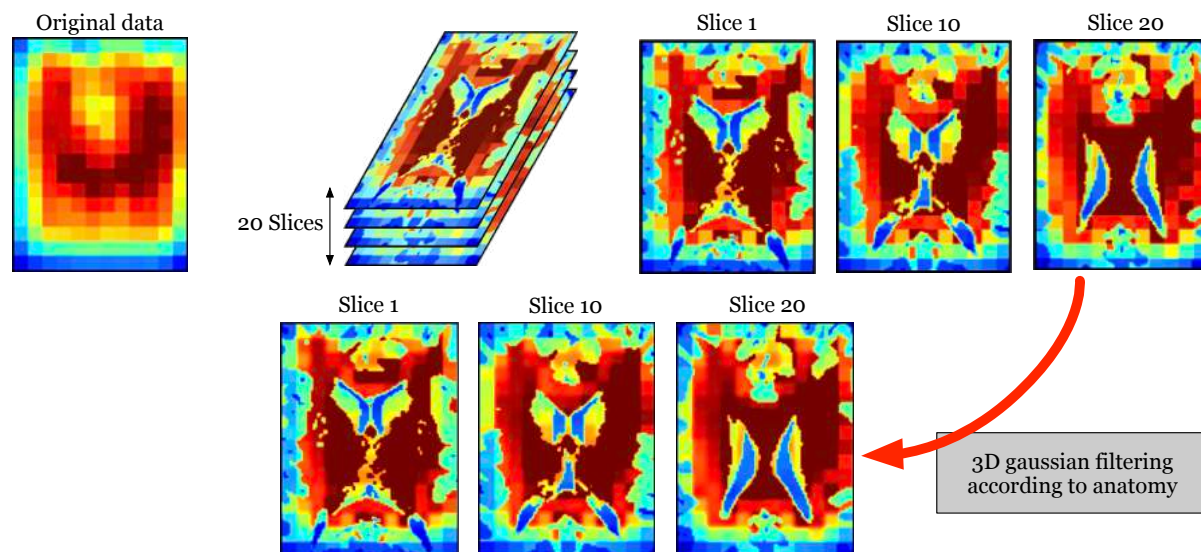


Figure 5: Results of our process: molecular concentration distribution in the segmentation grid taking into account the nature of the underlying tissues. A 3D gaussian filtering is applied to improve the final visualization.

	Choline (CHO)		Creatine (Cr)		N-acetylaspartate (NAA)	
	Gray matter	White matter	Gray matter	White matter	Gray matter	White matter
Clinical studies	1.8 ± 0.4	2.7 ± 0.5	11.3 ± 1.4	10.3 ± 1.2	15.7 ± 1.5	17.6 ± 1.6
Our method	1.5 ± 0.4	2.6 ± 0.5	11.1 ± 1.5	10.2 ± 1.3	15.7 ± 1.6	17.4 ± 1.5

Table 1: Comparison of concentration variations estimated by our method with those described in [21] for three molecules: Choline (CHO), Creatine (Cr) and N-acetylaspartate (NAA), present in white matter and gray matter (unit is $mmol.Kg^{-1}$).

4 APPLICATION ON A TUMOR SUBJECT

As mentioned in Sec. 1, the concentrations of molecules obtained using advanced magnetic resonance imaging technique can be useful for distinguishing healthy tissue from tumor tissue by applying simple thresholding and for determining the grade of a tumor by studying the variation of this concentrations in the volume

affected by the disease [20]. However, the low spatial resolution of the acquisition grid of this magnetic resonance imaging technique may affect the detection of tumor type and its localization in the brain. When the macrovoxel size is larger, the spatial resolution is reduced, making it more difficult to identify small tumors and to distinguish tumors from healthy tissues in a disease-affected scan volume. The existing methods to visualize these concentrations do not ensure an overall view of the tumor since they apply basic operations that do not take into account the nature of the tissues. These methods lack the ability to accurately pinpoint the location of brain tumors and assess the concentration of molecules in the tumor area. This makes it challenging to precisely determine the grade of the tumor (Fig. 6). Therefore, it is recommended to use this magnetic resonance imaging technique in combination with higher resolution anatomical imaging techniques obtained after application of the segmentation method in a tumor subject to improve the diagnosis and treatment of tumor tissues.

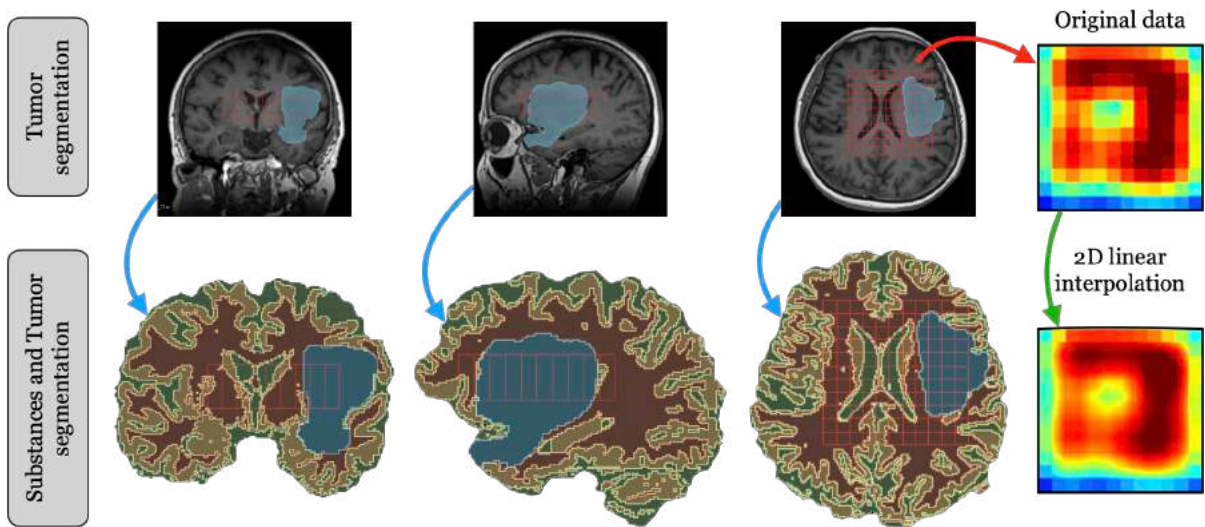


Figure 6: Three views of acquisition grid [red colored] on a T1 MRI slice of tumor subject with the tumor region [blue colored]; Three views of acquisition grid [red colored] on a MRI slice segmented into three brain substances: cerebrospinal fluid mask [green colored], white matter mask [brown colored] and gray matter mask [yellow colored] with the tumor region [blue colored]; The concentration distribution in the acquisition grid and that in the segmentation grid after applying the linear interpolation on the estimated concentration values (standard method presented in Sec 2): from the higher concentration [dark red colored] to the lower concentration [dark blue colored].

In order to address the limitations of the existing methods and of the low resolution acquisition grid, high resolution anatomical images obtained after the segmentation process should be considered. For a subject with a tumor, the segmentation process decomposes the brain into four classes, which include the three brain substances (WM, GM, and LSC) as well as the tumor area. While the segmentation process can determine the location of the tumor zone, it is not possible to determine its type or grade. The process can only provide information about its position and volume (Fig. 6). In the acquisition grid, macrovoxels that do not contain tumors can be assumed to be healthy and analyzed using the same steps described in Sec 3. However, macrovoxels that contain a certain tumor volume will have a fourth partial volume representing the tumor volume. The algorithm cannot be directly applied to these macrovoxels. It is thus important to extend our algorithm to deal with tumor regions. In the following, we explain the algorithm applied on a tumor macrovoxel.

For each macrovoxel containing tumor tissue, the mass of the molecule X is distributed over four volumes: V_1 , V_2 , V_3 and V_4 . The volumes V_1 , V_2 and V_3 represent the volumes of three brain substances in this macrovoxel which are healthy tissues, while V_4 represents the volume of the tumor (Fig. 6). The concentration of the molecule X in the tumor, denoted C_4 , is unknown and depends on the type of tumor and its grade. There are several types of brain tumors and the metabolic profile of each type can vary greatly (concentration values of a set of molecules) [8]. Therefore we cannot link C_4 to the other concentrations of healthy cerebral substances. The mass of the molecule X for a tumor macrovoxel is equal to $C * V$. This mass is non-uniformly distributed between the three brain substances and the tumor for this macrovoxel but it is always conserved (Eq. 6).

$$C * V = C_1 * V_1 + C_2 * V_2 + C_3 * V_3 + C_4 * V_4 \quad (6)$$

To maintain tumor characteristics, it is assumed that the C_4 concentration is always unknown and must be initialized according to other concentrations in healthy tissues of this macrovoxel. For this, it is first necessary to initialize the concentrations C_1 , C_2 and C_3 . By applying our algorithm to a healthy subject, we have noticed that the concentration values are related not only to the type of tissue but also to the location of the macrovoxel in the brain. Then the molecular concentration of the three cerebral substances for a tumor macrovoxel is estimated by averaging, for each substance, the concentration of neighboring healthy macrovoxels. This method respects the fact that the concentration value of X is provided by the nature of the tissues and the positioning in the brain. After having initialized the concentrations in the healthy tissues of the tumor macrovoxel, we can estimate the concentration of X in the tumor region using the following equation:

$$C_4 = \frac{C * V - (C_1 * V_1 + C_2 * V_2 + C_3 * V_3)}{V_4} \quad (7)$$

After estimating the concentration of a molecule X in each volume V , we make the assumption that X is evenly distributed within each volume, and we initialize the concentration of X in each microvoxel by the concentration value C_i estimated in the macrovoxel, which were determined based on the nature of the tissue. The concentration of X in each microvoxel of volume V_i is then set to C_i . The results of our modeling method applied to a tumor subject are shown in Fig. 7.

5 DISCUSSION

Partial volume effects have the disadvantage of introducing errors when quantifying molecular concentrations in a well-localized brain volume. This occurs because the resolution of the imaging technique is not high enough to differentiate between the tissues or substances within the macrovoxel that contains a mixture of multiple brain substances. Usual methods for visualizing these concentrations do not take into account the impact of partial volumes on the molecular distribution inside the acquisition volume. Consequently, the accuracy of the represented models is limited by the coarse sampling of the acquisition grid, leading to inaccuracies in the process of quantifying molecular concentrations. To address these limitations, we have developed a multimodal method of molecular concentration modeling which better distributes the molecular concentrations by taking into account the actual nature of the underlying tissues based on distribution rates assessed by clinical studies [21].

A new visualization technique has been developed in the open-source software 3D Slicer [5] that offers significant advantages over traditional methods. This technique provides higher spatial resolution, generating a more accurate concentration distribution and providing a more complete view of the tissues. This is particularly crucial for detecting subtle differences in the concentration of brain substances that might be missed by conventional methods. Our approach takes into account the specific characteristics of the visualized data according to the nature of the tissues, such as the quantitative parameters measured after the acquisition. The results show a variation of the concentrations according to the depth of the voxel: this variation depends

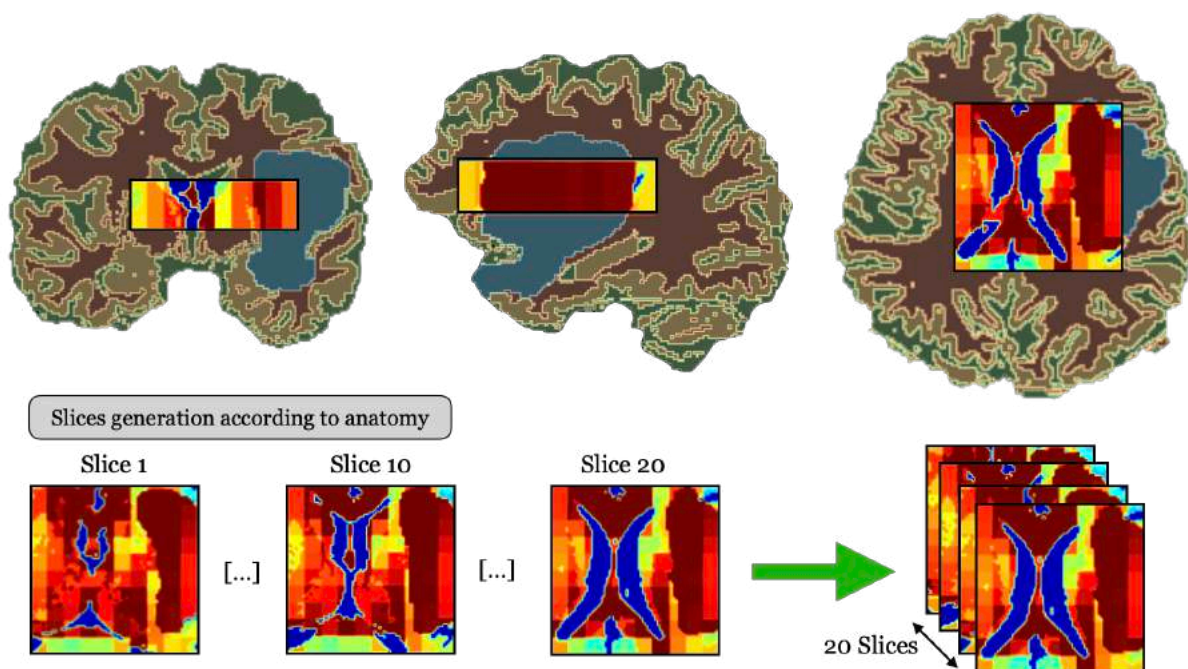


Figure 7: Three views of the molecular concentration slices in the segmentation grid with the corresponding brain substance masks and tumor region after applying our method. Molecular concentration distribution in the segmentation grid take into account the nature of the underlying tissues.

on the nature of the tissues, unlike conventional methods where the same concentration value on all the depth of a macrovoxel for a 2D position in the segmentation grid. In this context, our method offers a new tool to model dynamically and in 3D the concentrations of molecules in the brain according to the distribution rates selected by the doctors.

The output of the algorithm was subjected to Gaussian filtering. This technique can be useful in scenarios where the image is marred by noise or other unwanted features that may occur during the segmentation process in a clinical setting. This filtering is done by substance so that it does not affect the concentration values of the other substances. The purpose of applying Gaussian filtering is to smooth the image and remove any unwanted noise or artifacts, improving the clarity of the end result.

To validate the results obtained from our method, a study was conducted to analyze the variations of concentrations in each brain substance after applying our method. The results indicate that each molecule is distributed within a defined range in each substance. The small variations observed within each substance can be attributed to the position of the acquisition volume in the brain. Our results are consistent with previous studies in the literature and demonstrate that the concentrations in each substance are well-matched.

We have developed an algorithm that allows to visualize accurately changes in molecular concentrations within a tumor volume. By combining anatomical data with the advanced MRI acquisition, we can simultaneously utilize their respective strengths: the segmentation process provides precise spatial resolution to identify tumor area, but it cannot determine tumor type or grade. On the other hand, advanced MRI acquisition can determine the metabolic profile of the well-located volume in the brain affected by a tumor, which can help to identify the type and evolution of the tumor, although its effectiveness is limited in because of its low spatial resolution. Our method merges these two types of acquisition to detect changes in the concentrations

of molecules in the tumor volume. This provides a comprehensive view of the tumor, which is especially important for clinicians treating patients with complex or aggressive tumors.

Despite these improvements, it should be noted that there are limitations in terms of spatial resolution. One cannot refine acquisition volumes in voxels smaller than segmentation voxels, which limits the degree of resolution improvement we can achieve after applying our algorithm. Therefore, our ability to improve the spatial resolution is limited by the spatial resolution of the segmentation grid. Increasing the resolution of the segmentation grid is difficult due to challenges posed by limitations in imaging technology, variability in brain anatomy, and limited knowledge of brain tissue properties. Although the segmentation grid represented by voxels of $1 \times 1 \times 1 \text{ mm}^3$ may seem limited, it is generally adequate for most purposes. This level of resolution allows for highly detailed visualization, providing clinicians with the information needed to effectively diagnose and treat brain diseases.

6 CONCLUSION AND PERSPECTIVES

In this work, we have proposed a new method for 3D modeling and multimodal visualization of medical data. This approach allows a more accurate modeling and distribution of molecular concentrations by taking into account the actual composition of the underlying tissues based on distribution rates determined by clinical studies. This method can improve the accuracy of measurements by accounting for the partial volume effect that hides important information for surgeons. Existing methods for visualizing and refining this type of data are not able to completely deal with. This new method provides thus more reliable data for diagnosis and treatment planning. One of the perspectives of this work is to integrate other advanced imaging techniques such as perfusion and diffusion data with anatomical data, in a single and coherent visual representation. The combination of these types of data increases the sensitivity, specificity, and accuracy for the clinicians and for researchers in their diagnoses. Such complete multimodal visualisation will allow a better understanding of the underlying physiological processes, an improvement in the recognition of grade of gliomas and an enhancement in treatment planning providing a more complete picture of the patient's condition.

ACKNOWLEDGEMENTS

This research is funded by Region Nouvelle-Aquitaine, France and SIEMENS Healthineers.

REFERENCES

- [1] Abdelgawad, M.; Kayed, M.; Reda, I.; Abdelzaher, E.; Farhoud, A.; Elsebaie, N.: Contribution of advanced neuro-imaging (mr diffusion, perfusion and proton spectroscopy) in differentiation between low grade gliomas gii and mr morphologically similar non neoplastic lesions. *Egyptian Journal of Radiology and Nuclear Medicine*, 53(1), 2022. ISSN 2090-4762. <http://doi.org/10.1186/s43055-022-00695-2>.
- [2] Al-Iedani, O.; Lechner-Scott, J.; Ribbons, K.; Ramadan, S.: Fast magnetic resonance spectroscopic imaging techniques in human brain- applications in multiple sclerosis. *Journal of biomedical science*, 24(1), 17, 2017. ISSN 1021-7770. <http://doi.org/10.1186/s12929-017-0323-2>.
- [3] Bhima, K.; Jagan, A.: Analysis of mri based brain tumor identification using segmentation technique. In 2016 International Conference on Communication and Signal Processing (ICCSP), 2109–2113, 2016. <http://doi.org/10.1109/ICCSP.2016.7754551>.
- [4] Buonocore, M.H.; Maddock, R.J.: Magnetic resonance spectroscopy of the brain: a review of physical principles and technical methods. *Reviews in the Neurosciences*, 26(6), 609–632, 2015. <http://doi.org/doi:10.1515/revneuro-2015-0010>.

- [5] Diaz, O.; Kushibar, K.; Osuala, R.; Linardos, A.; Garrucho, L.; Igual, L.; Radeva, P.; Prior, F.; Gkontra, P.; Lekadir, K.: Data preparation for artificial intelligence in medical imaging: A comprehensive guide to open-access platforms and tools. *Physica medica*, 83, 25–37, 2021. ISSN 1120-1797.
- [6] Fawzi, A.; Achuthan, A.; Belaton, B.: Brain image segmentation in recent years: A narrative review. *Brain Sciences*, 11(8), 1055, 2021. ISSN 2076-3425. <http://doi.org/10.3390/brainsci11081055>.
- [7] Fellah, S.; Caudal, D.; De Paula, A.; Dory-Lautrec, P.; Figarella-Branger, D.; Chinot, O.; Metellus, P.; Cozzone, P.; Confort-Gouny, S.; Ghattas, B.; Callot, V.; Girard, N.: Multimodal mr imaging (diffusion, perfusion, and spectroscopy): is it possible to distinguish oligodendroglial tumor grade and 1p/19q codeletion in the pretherapeutic diagnosis? *AJNR. American journal of neuroradiology*, 34(7), 1326–1333, 2013. ISSN 0195-6108. <http://doi.org/10.3174/ajnr.a3352>.
- [8] Hampton, D.G.; Goldman-Yassen, A.E.; Sun, P.Z.; Hu, R.: Metabolic magnetic resonance imaging in neuroimaging: Magnetic resonance spectroscopy, sodium magnetic resonance imaging and chemical exchange saturation transfer. *Seminars in Ultrasound, CT and MRI*, 42(5), 452–462, 2021. ISSN 0887-2171. <http://doi.org/https://doi.org/10.1053/j.sult.2021.07.003>.
- [9] Hamsini, B.C.; Reddy, B.N.; Neelakantan, S.; Kumaran, S.P.: Clinical application of mr spectroscopy in identifying biochemical composition of the intracranial pathologies. In J. Samardzic, ed., *GABA And Glutamate*, chap. 7. IntechOpen, 2018. ISBN 978-953-51-3821-1. <http://doi.org/10.5772/intechopen.71728>.
- [10] Jia, Z.; Chen, D.: Brain tumor identification and classification of mri images using deep learning techniques. *IEEE Access*, 1–1, 2020. <http://doi.org/10.1109/ACCESS.2020.3016319>.
- [11] Lachanis, S.B.; Papachristos, I.E.: *Advanced MRI Techniques in Brain Tumors*, 169–176. Springer International Publishing, 2018. ISBN 978-3-319-68873-2. http://doi.org/10.1007/978-3-319-68873-2_20.
- [12] Lepcha, D.C.; Goyal, B.; Dogra, A.; Goyal, V.: Image super-resolution: A comprehensive review, recent trends, challenges and applications. *Information Fusion*, 91, 230–260, 2023. ISSN 1566-2535. <http://doi.org/https://doi.org/10.1016/j.inffus.2022.10.007>.
- [13] Mohd Sagheer, S.V.; George, S.N.: A review on medical image denoising algorithms. *Biomedical Signal Processing and Control*, 61, 102036, 2020. ISSN 1746-8094. <http://doi.org/https://doi.org/10.1016/j.bspc.2020.102036>.
- [14] Padelli, F.; Mazzi, F.; Erbetta, A.; Chiapparini, L.; Doniselli, F.; Palermo, S.; Aquino, D.; Bruzzone, M.; Cuccharini, V.: In vivo brain mr spectroscopy in gliomas: clinical and pre-clinical chances. *Clinical and Translational Imaging*, 10(5), 495–515, 2022. <http://doi.org/10.1007/s40336-022-00502-y>.
- [15] Pan, J.; Twieg, D.; Hetherington, H.: Quantitative spectroscopic imaging of the human brain. *Magnetic resonance in medicine*, 40(3), 363–369, 1998. ISSN 0740-3194. <http://doi.org/10.1002/mrm.1910400305>.
- [16] Quadrelli, S.; Mountford, C.; Ramadan, S.: Hitchhiker’s guide to voxel segmentation for partial volume correction of in vivo magnetic resonance spectroscopy. *Magnetic Resonance Insights*, 9, 1–8, 2016. <http://doi.org/10.4137/MRI.S32903>.
- [17] Singh, M.K.; Singh, K.K.: A review of publicly available automatic brain segmentation methodologies, machine learning models, recent advancements, and their comparison. *Annals of Neurosciences*, 28(1-2), 82–93, 2021. <http://doi.org/10.1177/0972753121990175>.
- [18] Tal, A.; Kirov, I.I.; Grossman, R.I.; Gonen, O.: The role of gray and white matter segmentation in quantitative proton mr spectroscopic imaging. *NMR in biomedicine*, 25(12), 1392–1400, 2012. ISSN 0952-3480. <http://doi.org/10.1002/nbm.2812>.
- [19] Vadmal, V.; Junno, G.; Badve, C.; Huang, W.; Waite, K.A.; Barnholtz-Sloan, J.S.: MRI image analysis

- methods and applications: an algorithmic perspective using brain tumors as an exemplar. *Neuro-Oncology Advances*, 2(1), 2020. ISSN 2632-2498. <http://doi.org/10.1093/noajnl/vdaa049>.
- [20] Weinberg, B.; Kuruva, M.; Shim, H.; Mullins, M.: Clinical applications of magnetic resonance spectroscopy in brain tumors. *Radiologic Clinics of North America*, 59(3), 349–362, 2021. <http://doi.org/10.1016/j.rcl.2021.01.004>.
- [21] Wright, A.M.; Murali-Manohar, S.; Henning, A.: Quantitative t1-relaxation corrected metabolite mapping of 12 metabolites in the human brain at 9.4 t. *NeuroImage*, 263, 119574, 2022. ISSN 1053-8119. <http://doi.org/https://doi.org/10.1016/j.neuroimage.2022.119574>.